Angular and Energy Correlations in the Reaction $O^{16}(\alpha,2\alpha)C^{12}_{g.s.}$ at 40-MeV Incident Alpha-Particle Energy*†

P. F. DONOVAN, J. V. KANE, AND Č. ZUPANČIČ‡
Bell Telephone Laboratories, Murray Hill, New Jersey, and Brookhaven National Laboratory, Upton, New York

AND

C. P. BAKER AND J. F. MOLLENAUER
Brookhaven National Laboratory, Upton, New York

(Received 26 November 1963)

The correlations in energy and angle of alpha particles produced in the reaction $O^{16}(\alpha,2\alpha)C^{12}_{g.s.}$ have been measured. Coincidence techniques were employed using semiconductor particle detectors and two-dimensional pulse-height analysis. The data show that a two-step reaction mechanism involving the formation and decay of excited states of O^{16} plays an important role. However, direct knock-out features of the reaction are also prominent and appear to be inextricably interwoven with its two-step aspects.

I. INTRODUCTION

IN an attempt to describe quantitatively a complicated nuclear reaction such as the one treated in this paper, drastic approximations are inevitable. The first and most natural of these is to consider the incident and outgoing particles as elementary. Even so, one is left with a three-body problem which has not yet been solved.

There are two widely used approximations which reduce the three-body problem to a manageable calculation. One is the application of direct reaction theory in its various degrees of sophistication, which is expected to give reasonably correct results at high energies. On the other hand, at low energies the reaction may proceed in at least two independent steps (for instance, via excitation of the target nucleus and its subsequent decay), each of which is simpler and better understood than the general reaction mechanism. This description of the reaction process should be adequate in cases when the intermediate system exists in a well-defined stationary state for a time interval which is long compared to characteristic nuclear traversal times. Even so, there remains the problem of understanding the ever present, and in general interfering, background of processes of a more general type. In the past, experimental results have been analyzed in many cases by assuming that the reaction proceeds partially via intermediate states (to the extent that resonance structure is present) and partially by some "direct" process. It is clear that an uncritical application of such subtraction procedures to experimental data, based on the assumption of no coherence between the two processes, could lead to erroneous conclusions.

Recent theoretical developments[1] have yielded a unified theory of nuclear reactions which encompasses both extreme approximations mentioned above. This theory is in principle capable of treating the interesting intermediate situations which are most often encountered in nature. However, for reactions producing three nuclei in the final state, the lack of understanding of the three-body problem is an especially serious obstacle to further progress. Detailed experimental studies of a number of such reactions may reveal empirical regularities which would constitute useful guides for the necessarily approximate theoretical treatment.

One might expect the reaction $O^{16}(\alpha,2\alpha)C^{12}_{g.s.}$ at 40-MeV incident alpha-particle energy to proceed to a great extent via excited states of O^{16} above the 7.16-MeV threshold for decay into $C^{12}_{g.s.}$ and an alpha particle. Some of these states, especially those near the threshold, are known to be quite long lived[2] and therefore a description in terms of a two-step process of the part of the reaction which proceeds via these sharp states should be reasonably accurate.

A simple but sensitive criterion for the accuracy of the two-step description is provided by the angular correlation between the first (inelastically scattered) alpha particle, and the second alpha particle (emitted in the subsequent decay of the excited O^{16} state). If this state is sufficiently long-lived that the excitation process is, on the average, well-separated in time from the decay process, and if the state is isolated, i.e., possesses a well-defined spin and parity, one can apply the selection rule of A. Bohr[3] to derive the following statement about the angular correlation (see Appendix I for details): In the rest system of the excited O^{16} nucleus, the normal to the

* Work performed in part under the auspices of the U. S. Atomic Energy Commission.

† Part of the results of the work described in this paper have been previously reported in the Bull. Am. Phys. Soc. **7**, 287 (1962) and the *Proceedings of the International Conference on Direct Interactions and Nuclear Reaction Mechanisms, Padua* (Gordon and Breach, New York, 1963), p. 1050.

‡ Presently at the University of Ljubljana and the Institute "J. Stefan," Ljubljana, Yugoslavia.

[1] G. E. Brown, Rev. Mod. Phys. **31**, 893 (1959); J. Humblet and L. Rosenfeld, Nucl. Phys. **26**, 529 (1961); H. Feshbach, Ann. Phys. (N. Y.) **5**, 357 (1958) and **19**, 287 (1962); E. Vogt, Rev. Mod. Phys. **34**, 723 (1962). (See these papers for other references.)

[2] T. Lauritsen and F. Ajzenberg-Selove, in *Nuclear Data Sheets*, compiled by K. Way *et al.* (Printing and Publishing Office, National Academy of Sciences, Washington, D. C., 1962). NRC 61-5, 6-3.

[3] A. Bohr, Nucl. Phys. **10**, 486 (1959).

scattering plane (defined by the incident beam and the direction of the inelastically scattered alpha particle) is an axis of twofold symmetry of the angular pattern of the second alpha particle. This means that for any given direction of the first alpha particle, the correlation pattern starts repeating itself after the detector registering the second alpha particle has moved 180° (as seen from the recoiling O^{16} nucleus) around the normal to the scattering plane. This statement is true as long as the above assumptions are fulfilled, independent of the specific spin-parity value of the intermediate state and independent of mechanism of the formation of the state. It should be made precise by defining a sufficiently long-lived state. This would be possible in terms of the characteristic nuclear traversal time, which provides a time gauge, were it not for Coulomb forces. However, even in the presence of Coulomb forces, those states which live much longer than a nuclear traversal interval should be little perturbed and the above statement concerning the correlation pattern should be at least approximately correct.

In general, the normal to the scattering plane ceases to be an axis of twofold symmetry for the correlation if two or more intermediate states of opposite parity overlap and interfere. The symmetry might be restored in cases where the contributions of many intermediate states have been added together, if their phases are randomly distributed. However, when the overlap of intermediate states becomes the rule rather than the exception, a completely random phase distribution can hardly be expected. The coupling between the different modes of internal nuclear motion necessitates a linkage of phases. It is expected that direct reaction features should emerge from such phase correlations. Moreover, when intermediate states overlap as a rule, in many cases the whole reaction takes place within a nuclear traversal interval. This means that the distinction between the first and second alpha particle becomes operationally meaningless and the whole concept of a two-step process breaks down. It then becomes unavoidable to consider the three-body nature of the reaction in its full complexity.

In order to obtain the simple alpha angular-correlation pattern which would be predicted by a two-step reaction mechanism in the case of the reaction $O^{16}(\alpha,2\alpha)C^{12}_{g.s.}$, the overlapping of different intermediate states must not be too important. Although there are many narrow alpha-emitting states in the investigated energy region of O^{16}, there are also known broad states, some of which are not far removed from the threshold for alpha emission. The overlap of such broad levels is expected to become even worse at higher excitation energies, and coherent contributions from the tails of high-lying broad states may be important even at low excitation energies. The angular-correlation pattern can therefore hardly be expected to possess the exact symmetry property discussed above. However, the interplay of intermediate states with nonrandom phases and specific three-body effects may lead to some simple regularities which could not easily be predicted but could perhaps be theoretically explained *a posteriori*. Such explanations could then lead to further progress in the three-body problem. Also, they might enable us to extract from experimental data two-body parameters, such as energies, spins, and parities of intermediate states, in spite of specific three-body aspects of the reaction. It was for these reasons that this experiment was undertaken.

The experimental method used in the present investigation had some novel features. The coincident angle and energy determination of both outgoing alpha particles with two solid-state detectors leaves no room for kinematic ambiguities: The final state is completely determined by the measurement. Further, the use of two-dimensional pulse-height analyzers permits a data taking speed and comparative ease of analysis which were previously impossible.

II. KINEMATICS

In the reaction $O^{16}(\alpha,2\alpha)C^{12}_{g.s.}$ all ingoing and outgoing particles have zero spin. Both the initial and final states of the reaction are therefore completely characterized by the ingoing and outgoing particle momenta, which are related by the conservation of momentum and energy. In the nonrelativistic approximation we have

$$\mathbf{p}_1+\mathbf{p}_2=\mathbf{p}_3+\mathbf{p}_4+\mathbf{p}_5, \tag{1}$$

$$T_1+T_2+Q=T_3+T_4+T_5, \tag{2}$$

$$T_i=p_i^2/2m_i, \tag{3}$$

$$Q=(m_1+m_2-m_3-m_4-m_5)c^2, \tag{4}$$

m_i being the mass of particle i, $\mathbf{p}_i$ its momentum, and T_i its kinetic energy. We designate the incident particle by the index 1, the target nucleus by the index 2, while the indices 3, 4, and 5 label the outgoing particles. Q is the Q value of the reaction and c the velocity of light. Equations (1)–(4) are valid in any inertial system. In the laboratory system we have $\mathbf{p}_2=0$. Equations (1)–(4) considerably reduce the number of independent variables needed to specify the final state. Conservation of momentum (1) enables us to express the momentum of one outgoing particle, for example $\mathbf{p}_5$, by the momenta of the ingoing particles $\mathbf{p}_1$ and $\mathbf{p}_2$ and the momenta of the other two outgoing particles $\mathbf{p}_3$ and $\mathbf{p}_4$. From (2) and (3) one then obtains

$$T_1+T_2+Q=T_3+T_4+\frac{(\mathbf{p}_1+\mathbf{p}_2-\mathbf{p}_3-\mathbf{p}_4)^2}{2m_5}$$
$$=T_3+T_4+\frac{(\mathbf{p}_1+\mathbf{p}_2-\mathbf{p}_3-\mathbf{p}_4)^2}{2(m_1+m_2-m_3-m_4)}. \tag{5}$$

The substitution $m_5=m_1+m_2-m_3-m_4$ in the denominator of the last term is entirely in the spirit of the nonrelativistic approximation since the Q value is much

smaller than any m_ic^2. Equation (5) determines the Q value if all momenta are known. Conversely, for a definite Q value and a definite initial state, it establishes a relation among the six variables needed to specify the vectors $\mathbf{p}_3$ and $\mathbf{p}_4$, and therefore reduces to five the number of independent variables characterizing the final state of the reaction. These variables may be chosen, for example, to be the polar angles θ_3, ϕ_3, θ_4, and ϕ_4 characterizing the directions of the two vectors $\mathbf{p}_3$ and $\mathbf{p}_4$, and the kinetic energy T_3.[4] Since in the laboratory system the reaction possesses axial symmetry around the direction of $\mathbf{p}_1$, the reaction cross section depends only on the difference between the azimuthal angles ϕ_3 and ϕ_4. At a given incident particle energy the cross section can therefore be expressed as a function of only four independent variables.

In the present experiment, complete kinematic determination of the final state and of the Q value of the reaction is achieved by using two energy-sensitive detectors in coincidence at specified angles with respect to the incident beam and the target. By this technique the variables T_3, T_4, θ_3, θ_4, and $(\phi_3-\phi_4)$ are determined for each event. A complete investigation of the reaction, i.e., a scanning of all three relevant angles θ_3, θ_4, and $(\phi_3-\phi_4)$ would require a prohibitive amount of time. Therefore the two detectors were restricted to a common plane with the incident beam line, fixing $(\phi_3-\phi_4)$. Furthermore, the data presented in this paper were taken with one detector fixed at an angle of 25° with respect to the incident beam direction.

The relationship between T_3 and T_4 as given by Eq. (5) is illustrated in Fig. 1 for the reaction $O^{16}(\alpha,2\alpha)C^{12}{}_{g.s.}$ at 40-MeV incident alpha-particle energy. Here particles 3 and 4 are the two emitted alpha particles, seen by two detectors on opposite sides of the beam at 25°.

The convention adopted here and in the following is to consider the angle of the fixed detector to be +25° with respect to the beam direction. The angle of the moving detector with respect to the beam direction is considered positive if the moving detector is on the same side of the beam as the fixed detector and negative if it is on the opposite side. Figure 1 is drawn with the origin of the coordinate system in the upper right corner in order to conform with analyzer memory displays presented later. All alpha-alpha coincidences leading to the formation of $C^{12}{}_{g.s.}$ must lie within the band in the figure. The finite width of the band is due to the angular spread of ±2.5° in each detector. A reaction with a lower Q value, e.g. $O^{16}(\alpha,2\alpha)C^{12}$ (first excited state) would appear on Fig. 1 as another band nearer the origin of the coordinate system. The reaction $O^{16}(\alpha,2\alpha)C^{12}{}_{g.s.}$ has the highest Q value of all reactions producing three or more outgoing particles which are possible with the given target and incident particle. Therefore in a coincidence measurement where both energies T_3 and T_4 are registered, the reaction $O^{16}(\alpha,2\alpha)C^{12}{}_{g.s.}$ is easily separated from other reactions. At some detector angles however, bands corresponding to alpha-C^{12} coincidences partially overlap the band representing the alpha-alpha coincidences. In such cases the C^{12} recoils were prevented from reaching the detectors by thin Al foils which stopped them without appreciably affecting the alpha particles of interest. Often the use of a target of sufficient thickness to emphasize the alpha-alpha band relative to the smeared-out alpha-C^{12} bands was found to be adequate. The separation of the alpha-alpha band from possible reactions producing only two outgoing particles is no serious problem, since such reactions are represented on T_3 versus T_4 diagrams of the type of Fig. (1) by spots which appear only at special angles. These angles can either be avoided or the recoil nuclei can be suppressed by suitable foils.

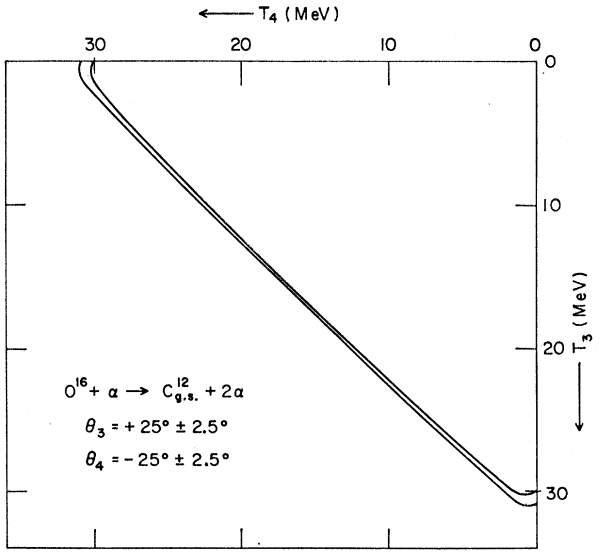

FIG. 1. A calculation of the allowed energies of alpha-alpha coincidences for the reaction O^{16}+40-MeV $\alpha \rightarrow C^{12}{}_{g.s.}+2\alpha$, with the indicated detector angles and angular apertures.

A strong final state interaction between two of the outgoing particles at a certain relative energy or its equivalent, the existence of a quasistationary intermediate system, manifests itself by the preferential population of some sections of the bands in the T_3 versus T_4 diagrams. If the intermediate system is formed by particles 4 and 5 (in our case an alpha particle and the C^{12} forming an O^{16} decaying state), the energy of particle 3 (the other alpha particle) is determined by the Q value of the reaction forming the intermediate system and by the angular position of detector 3.[5] In

[4] This selection of variables in general allows two values of T_4. However, this double value problem does not occur in the energy region of interest in this experiment.

[5] The labeling of the two alpha particles does not violate the principle of indistinguishability of identical particles. Particle 3 is simply the alpha particle registered by detector 3 and particle 4 the one registered by detector 4. The indistinguishability principle does prevent, for instance, the identification of either one of them with the incident alpha particle.

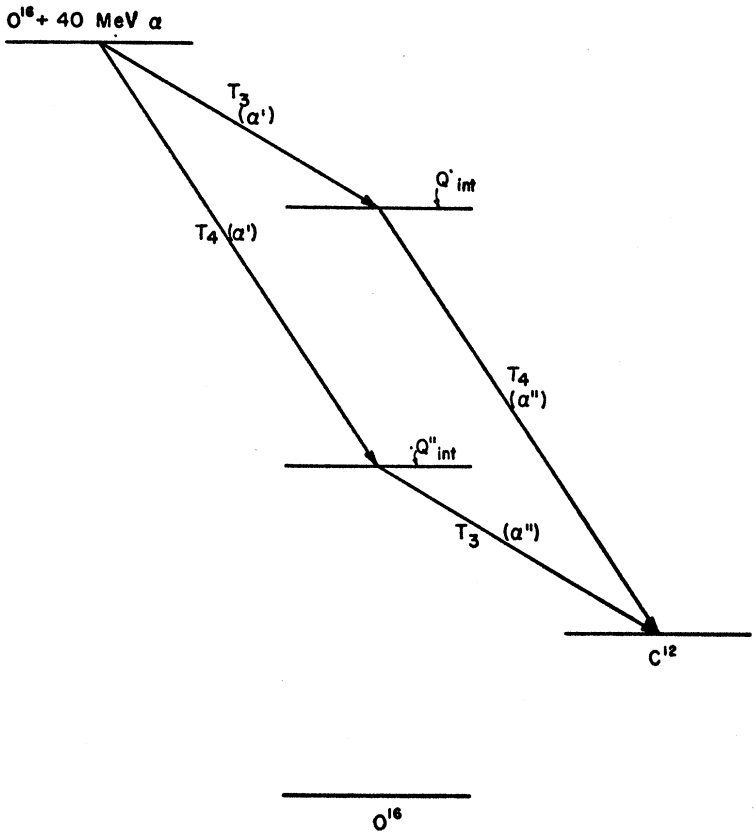

FIG. 2. An illustration of the ambiguity arising from the unknown time sequence of the two alpha particles corresponding to a particular spot on the alpha-alpha coincidence band at coordinates T_3 and T_4.

this case the reaction proceeds in two steps, the first of which is a reaction with two outgoing particles. Particle 3 takes part only in this step. The relevant equations are

$$\mathbf{p}_1+\mathbf{p}_2=\mathbf{p}_3+\mathbf{p}_{45}, \tag{6}$$

$$T_1+T_2+Q_{\text{int}}=T_3+T_{45}=T_3+\frac{(\mathbf{p}_1+\mathbf{p}_2-\mathbf{p}_3)^2}{2(m_1+m_2-m_3)}. \tag{7}$$

Here $\mathbf{p}_{45}$ is the momentum and T_{45} the kinetic energy of the intermediate system. Q_{int} is the Q value of the first step of the reaction and is necessarily smaller than the Q value of the whole reaction defined in Eq. (4).

On the other hand, if particles 3 and 5 form a quasi-stationary intermediate system, the energy of particle 4 is determined by Q_{int} and θ_4. The existence of a decaying state of O^{16} should therefore manifest itself by two spots with a large density of events on the alpha-alpha band. One spot corresponds to the case where the alpha particle emerging from the first step of the reaction is registered by detector 3 and the alpha particle from the decay of the intermediate system by detector 4. The other spot then arises from the opposite case. In the foregoing discussion, we have considered only the case in which the double-value problem mentioned in footnote 4 and the analogous problem for Eq. (7) do not occur. In this reaction there may, in general, be as many as eight spots on the alpha-alpha band from a single energy level in O^{16}, but only two occur in the energy region of interest here.

Conversely, the observation of a spot in the alpha-alpha band at any given pair of angles of the two detectors leaves an ambiguity (illustrated in Fig. 2) with respect to the value of Q_{int} since we do not know which of the two alpha particles emerged in the first step. The two possible assumptions about the sequence of the two alpha particles yield two possible values of Q_{int}. This ambiguity could in principle be resolved by time-delayed coincidence measurements. A more practical way of deciding the issue is to exploit the center-of-mass motion and observe the movement of the spots on the alpha-alpha band as the counter angles were varied. If one detector, e.g., detector 3, is left at a fixed angle and the angle of detector 4 is changed, those spots which correspond to alpha particles from the first step (α') entering detector 3 will retain their T_3 coordinate. On the other hand, the spots which correspond to alpha particles from the first step entering detector 4 will in general change both their T_3 and T_4 coordinates due to the center-of-mass motion. Figure 3 illustrates this for detector 3 at $\theta_3=+25°$ while detector 4 is moved from $\theta_4=-180°$ to $\theta_4=+180°$. The coordinate T_3 of the spot representing a decaying O^{16} state is plotted as a function of θ_4. The different bands correspond to different (hypothetical) decaying states of O^{16} with the indicated

values of Q_{int}. The width of the bands is again due to the $\pm 2.5°$ angular apertures of the detectors. The hypothetical states of O^{16} are assumed to be infinitely narrow. There are two families of bands (plotted separately for the sake of clarity), the straight bands representing the alpha particle from the first step (α') entering detector 3 and the curved bands representing the alpha particle from the decay of the intermediate system (α'') entering detector 3.

Apart from the fundamental requirement of narrow decaying states, the usefulness of an experimentally obtained plot of the type of Fig. 3 in deciding the time order of the outgoing particles has its practical limitations, owing to the finite precision of the measurements. It is most applicable in cases where the strongly populated particle decaying states are well separated in energy or when the lower-lying states are much more strongly populated than higher-lying ones. This latter manifests itself by the preponderance of straight bands at large values of T_3, while curved bands dominate at low values of T_3.

Let us now consider an intermediate system consisting of the two alpha particles (particles 3 and 4). This system corresponds to an alpha-decaying state of Be^8,

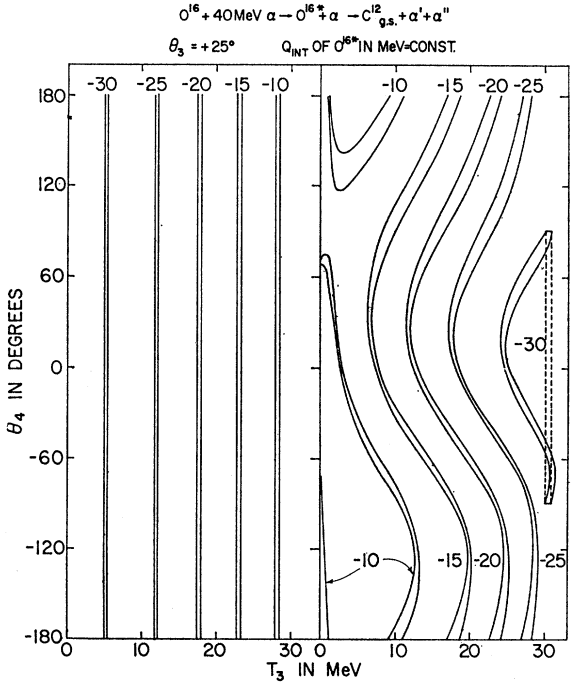

FIG. 3. Calculated energies T_3 of the alpha-particle registered in the detector at $+25°$ in coincidence with the other alpha particle detected at different angles θ_4 for various assumed values of Q_{int} (indicated in MeV). The two parts of the figure correspond to the two possible assumptions about the time sequence of the alpha particles. The dashed lines on the curve for $Q_{\text{int}}=-30$ indicate that although some laboratory angles are forbidden, the curve is closed in the $\alpha+O^{16}$ c.m. system and includes all c.m. angles.

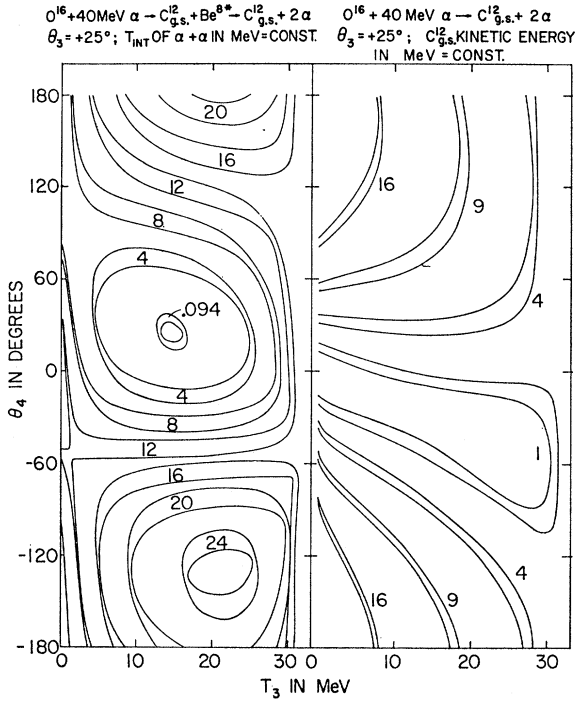

FIG. 4. Left side: A T_3 versus θ_4 diagram of the type to be expected if the reaction proceeds via alpha-decaying states of Be^8, calculated for the indicated values of T_{int} in MeV. Right side: A T_3 versus θ_4 diagram of the type to be expected if definite recoil energies T_5 (indicated in MeV units) are of importance in the reaction mechanism.

and is kinematically described by the equations

$$\mathbf{p}_{34}=\mathbf{p}_3+\mathbf{p}_4, \tag{8}$$

$$T_{34}+T_{\text{int}}=\frac{(\mathbf{p}_3+\mathbf{p}_4)^2}{2(m_3+m_4)}+T_{\text{int}}=T_3+T_4, \tag{9}$$

or

$$T_{\text{int}}=\frac{m_3m_4}{2(m_3+m_4)}\left(\frac{\mathbf{p}_3}{m_3}-\frac{\mathbf{p}_4}{m_4}\right)^2. \tag{10}$$

Here $\mathbf{p}_{34}$ is the momentum and T_{34} the kinetic energy of the intermediate system. T_{int} is the decay energy of the Be^8 intermediate system. On a diagram of the type of Fig. 3 the decay of states of Be^8 yields bands which are generally very broad due to the detector angular aperture, even for the case of infinitely narrow states of Be^8. These bands tend to run parallel to the T_3 axis of a T_3 versus θ_4 diagram, as shown in Fig. 4. This means that more or less the whole alpha-alpha band on a T_3 versus T_4 diagram is intensified at certain angles of the detectors. From this it is obvious that the measurement of the momenta of the two outgoing alpha particles is not the most suitable method for the extraction of information concerning decaying states of Be^8. The momenta of one alpha particle and of the C^{12} recoil nucleus should be measured instead, if one wishes to

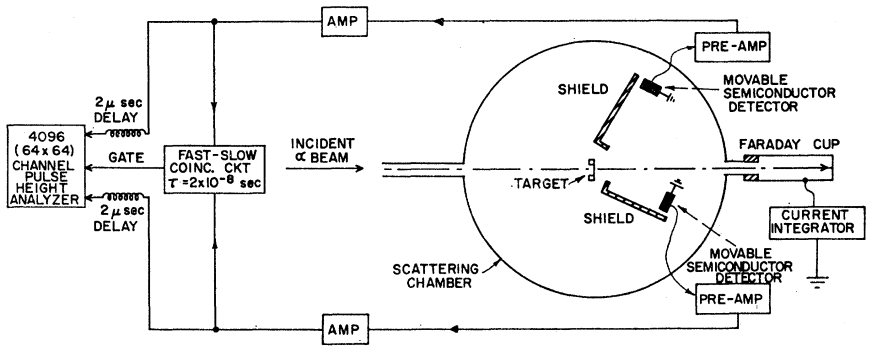

FIG. 5. A block diagram of the experimental apparatus.

emphasize those features of the reaction which depend on strong alpha-alpha final state interactions.

The second half of Fig. 4 presents T_3 versus θ_4 bands corresponding to a constant energy T_5 of the recoiling C^{12} nucleus. Their width is, again, due to the angular aperture of the detectors. This figure will be of interest in the comparison of the experimental data with the predictions of a direct knockout model.

Once the existence of a quasistationary intermediate system is demonstrated and the particles emitted in each step of the reaction are identified, it is of advantage to transform the relevant experimental data into the inertial system in which the intermediate nucleus is at rest. In such a coordinate system the symmetry theorem announced in the introduction is valid. The relevant formulas for the transformation of angles, energies, and products of solid angle and energy differentials are listed in Appendix II.

III. APPARATUS

A beam of 40-MeV He^{++} ions was obtained from the Brookhaven National Laboratory 60-in. cyclotron. This beam was analyzed by magnetic deflection through 45°. The horizontal focusing properties of the magnet were such that in the symmetric arrangement both the object and image plane were at about 1.7 m from the center of the magnet. The beam was geometrically defined by a 1-mm-wide entrance slit in the object plane and 1-mm circular aperture in the image plane. The strong angular dependence of the observed reaction necessitated a good definition of the angle of incidence on the target of the analyzed beam. This angle was frequently checked and also defined by a $\frac{1}{8}$-in. slit at the entrance of the beam into the magnetic field. The magnetic field was monitored by a nuclear magnetic-resonance fluxmeter which was calibrated against a BC-221 frequency meter. It is estimated that the energy spread and the energy reproducibility of the analyzed beam were about 100 keV. No attempts were made to determine the absolute value of the beam energy by magnetic-field measurements. However, the pulses produced in semiconductor detectors by alpha particles elastically and inelastically scattered from several targets and also by alpha particles from radioactive sources were compared to a linear pulser. They were consistent with an incident beam energy of 40.6±0.4 MeV. The large uncertainty in the absolute value of the energy is mainly due to the fact that only the rather small differences between the measured energies of the scattered particles are known absolutely, and the highest calibration energy from the radioactive source was only 5.48 MeV.

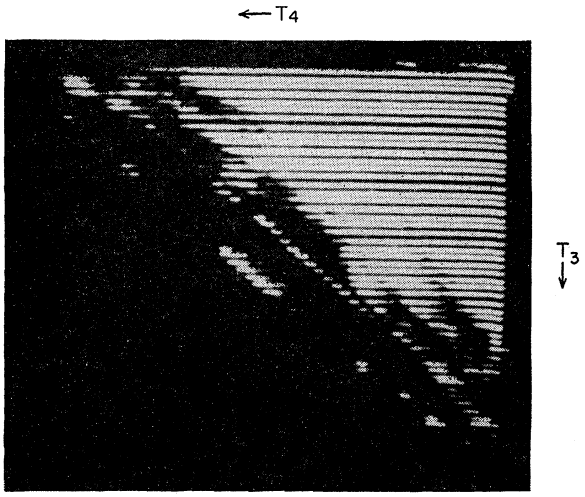

FIG. 6. A cathode-ray-tube display of raw data stored in the two-dimensional analyzer from the reaction $O^{16}(\alpha,2\alpha)C^{12}$ at detector angles $\theta_3=+25°$, $\theta_4=-25°$. See text for complete explanation of figure.

A block diagram of the experimental setup with the associated electronics is shown in Fig. 5. The analyzed beam entered a scattering chamber of 16-in. diameter which housed the target and two semiconductor detectors mounted on movable arms coplanar with the beam. The target was a thin SiO_2 foil. The thickness of the various SiO_2 foils used during the course of these experiments ranged from 0.1 to 1 mg/cm². The thickest of these contributed an effective maximum energy spread of about 200 keV to the incident beam. The effect on outgoing particles was more severe. An effort was made to minimize this effect by proper orientation of the target with respect to the direction of the outgoing particles; however, this procedure was usually useful only over a limited energy region. The thinner targets

were used whenever the low-energy alpha particles had to be well resolved. In general, however, uncertainties due to the target thickness were smaller than other experimental errors.

The detectors used in the experiment were made of p-type silicon with a diffused n-type layer of about 0.1 μ thickness on the front surface. The depletion layers were thick enough to stop 40-MeV alpha particles when the detector was inclined 45° with respect to the direction of incident particles. The detectors were made by us[6] and were of various shapes. Their areas were usually around 1 cm^2. They were positioned 1.5–6 cm from the target, providing angular apertures of about 3 to 12° in the horizontal direction and somewhat more in the vertical direction. The uncertainty in the positioning of the detectors, the wrinkles in the target, and the eccentricity of the beam caused an error in the absolute reading of the angles which was estimated to be at most 2°. The relative angle readings over a limited interval were considerably more accurate. The errors in solid angles, which had the same origin, were of the order of a few percent. Pulses from the detectors were amplified in conventional charge-integrating preamplifiers and double-delay-line clipped Cosmic-901 amplifiers. Whenever a coincidence event occurred this was recognized by a Cosmic-801 coincidence system, which gated a 64 by 64 (i.e., 4096) channel two-dimensional analyzer.[7] In this analyzer each of the two coincident pulses was digitized by analog to digital converters into 64 energy intervals. Then the event was stored in the appropriate location in the analyzer memory. The memory capacity is such that up to 2^{16} events can be stored in each of the 4096 channels of the 64-channel×64-channel array. The two-dimensional energy field of the analyzer can be displayed on a cathode-ray oscilloscope for visual inspection and photographic recording and also can be printed or punched on paper tape for quantitative data analysis. In this way a distribution of events in a T_3 versus T_4 diagram of the type of Fig. 1 was obtained by a single measurement.

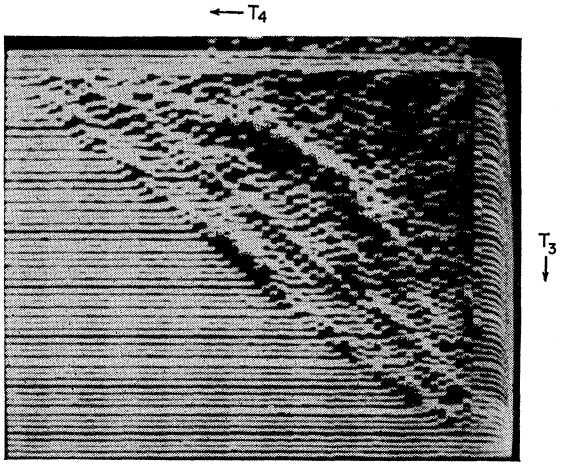

FIG. 7. A cathode-ray-tube display of raw data stored in the two-dimensional analyzer from the reaction $O^{16}(\alpha,2\alpha)C^{12}$ at detector angles $\theta_3=+25°$, $\theta_4=-25°$. See text for complete explanation of figure.

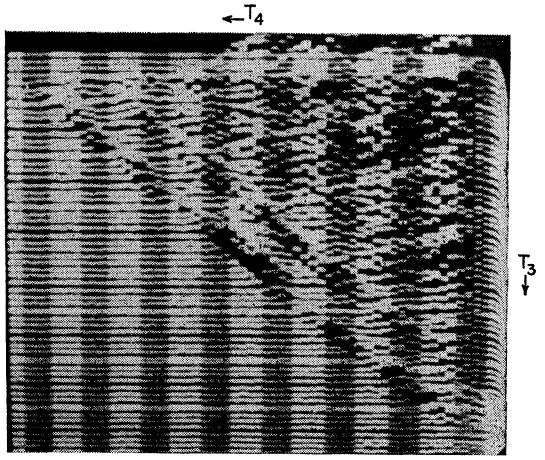

FIG. 8. A cathode-ray-tube display of raw data stored in the two-dimensional analyzer from the reaction $O^{16}(\alpha,2\alpha)C^{12}$ at detector angles $\theta_3=+25°$, $\theta_4=-25°$. See text for complete explanation of figure.

After passing through the target, the beam was stopped in a Faraday cup and the current integrated electronically. The integrator was periodically checked and found to be accurate to about 2%. All angular correlation measurements were done with this integrator as a monitor. This procedure was found satisfactory since the accuracy was more severely limited by other uncertainties, as will be seen.

IV. EXPERIMENTAL RESULTS

A cathode-ray-tube display of the data stored in the analyzer memory at the end of a 2-h run at the detector angles $\theta_3=+25°$, $\theta_4=-25°$ is shown in Fig. 6. The density of events is represented by the intensification of the cathode-ray-tube picture at the position determined by the coordinates T_3 on the vertical axis and T_4 on the horizontal axis. The origin of this coordinate system is in the upper right corner. The T_3 coordinate increases from top to bottom and the T_4 coordinate from right to left. The picture is taken with high contrast, i.e., the luminosity of the spots changes from 0 to maximum over a rather limited range of counts per channel. This makes some important features of the data very prominent. One sees the two alpha-alpha bands arising from the reactions $O^{16}(\alpha,2\alpha)C^{12}_{g.s.}$ and $O^{16}(\alpha,2\alpha)C^{12}$ first excited state. They are strongly intensity modulated, indicating the importance of intermediate decaying states of O^{16}. The broad bands nearer the origin are due to alpha-C^{12} coincidences. A more quantitative display is also available with the analyzer. It consists of a T_4 spectrum traced out for each single T_3 channel, with all 64 such

[6] P. F. Donovan, Natl. Acad. Sci.—Natl. Res. Council, Nucl. Sci. Ser. Rept. No. NAS-NS 32, 268 (1961).
[7] R. L. Chase, IRE Natl. Conv. Record 9, 196 (1959).

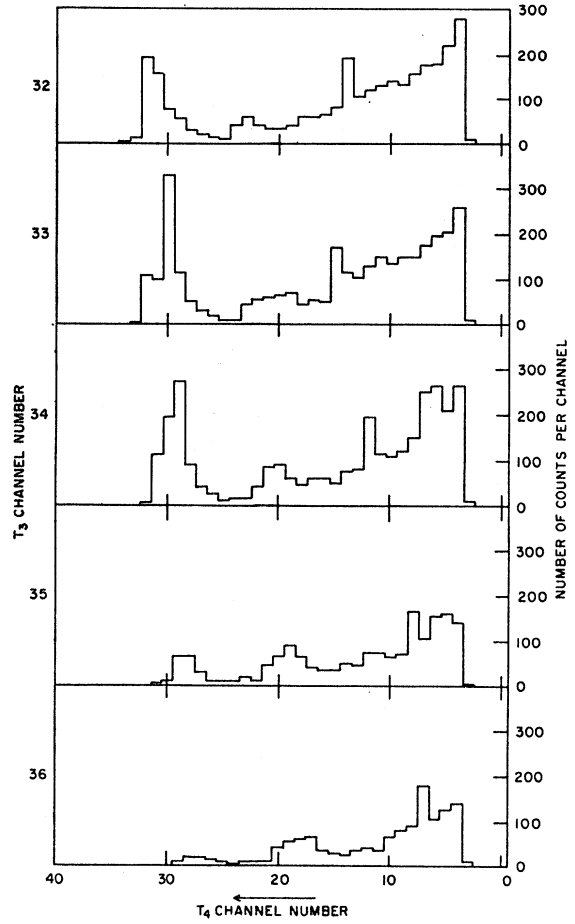

FIG. 9. A plot for several T_3 channels of the T_4 energy spectrum. These are raw data.

spectra displayed simultaneously while displaced from each other vertically a small amount. The same data shown in Fig. 6 are displayed in this way in Fig. 7. The origin of the coordinate system is again in the upper right corner. The coordinates T_3 and T_4 run as before, while the number of counts at each T_3, T_4 position is plotted vertically in units of 2^3 (2^{10} full scale). The vertical modulation bands, which are 4 channels wide, are introduced to facilitate the identification of the T_4 channel numbers. The data displayed in Figs. 6 and 7 were taken with a rather thin target and no foils in front of the detectors. The effect of a thicker target in de-emphasizing the alpha-C^{12} bands by stopping most of the C^{12} recoils is shown in Fig. 8, which represents data taken under otherwise identical conditions.

Part of the data presented in Fig. 8 is plotted in more detail in Fig. 9. The T_4 spectrum is plotted for each of five T_3 channels. It is seen that while the alpha-alpha band from the $O^{16}(\alpha,2\alpha)C^{12}{}_{g.s.}$ reaction is clearly separable from the rest of events, the density of events on the low-energy side of this band does not fall to zero. The origin of this phenomenon is not entirely understood. It is partly due to "tailing" in the counters, a phenomenon probably caused by edge effects and consisting of a low-energy tail following each peak in the spectrum. The ratio of peak height to tail height found in singles spectra was about 300. Since the tails were rather uniform this means that at a resolution of about 1% up to 25% of the total yield was in the tail. In a coincidence spectrum plotted on a T_3 versus T_4 diagram this effect is even more serious due to the addition of tails and double tailing.

Another contribution to the intensity in the valley between the bands belonging to the reactions $O^{16}(\alpha,2\alpha)C^{12}{}_{g.s.}$ and $O^{16}(\alpha,2\alpha)C^{12}$ first excited state was due to alpha-alpha coincidence from the reaction $Si^{28}(\alpha,2\alpha)Mg^{24}{}_{g.s.}$. Its Q value is -9.99 MeV, compared to -7.14 and -11.56 MeV for the first two reactions, respectively. At a few angles, alpha-alpha coincidences from the bombardment of a Si target by 40-MeV alpha particles were measured. The reaction $Si^{28}(\alpha,2\alpha)Mg^{24}$ could be detected but its contribution to the total yield from a SiO_2 target in the interesting energy range was estimated to be less than 5%.

After the raw data such as those presented in Fig. 9 were printed out, a quantitative separation of the contribution of the reaction $O^{16}(\alpha,2\alpha)C^{12}{}_{g.s.}$ was attempted in each case. Some "background" was subtracted from underneath the alpha-alpha band belonging to this reaction. The criteria for this subtraction were based on experience with many different spectra and were in this sense arbitrary. However, when the raw data were analyzed independently by different people, the results were the same within less than 10%, except possibly in regions of very small population of the alpha-alpha band. It is clear that in such a background subtraction procedure the contribution of the tail of the alpha-alpha

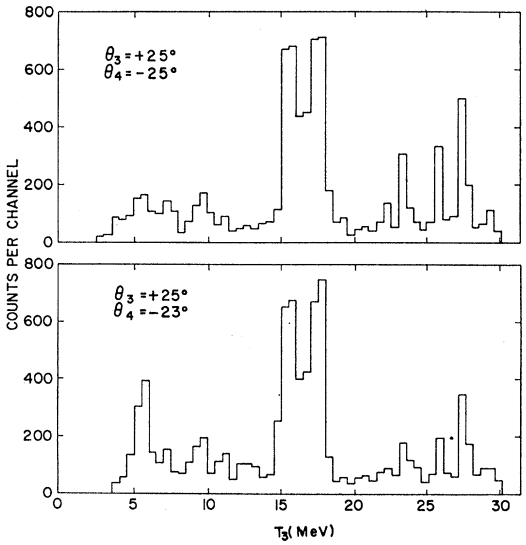

FIG. 10. T_3 spectra of the ground-state alpha-alpha band taken at two pairs of angles. See text for discussion of the figure.

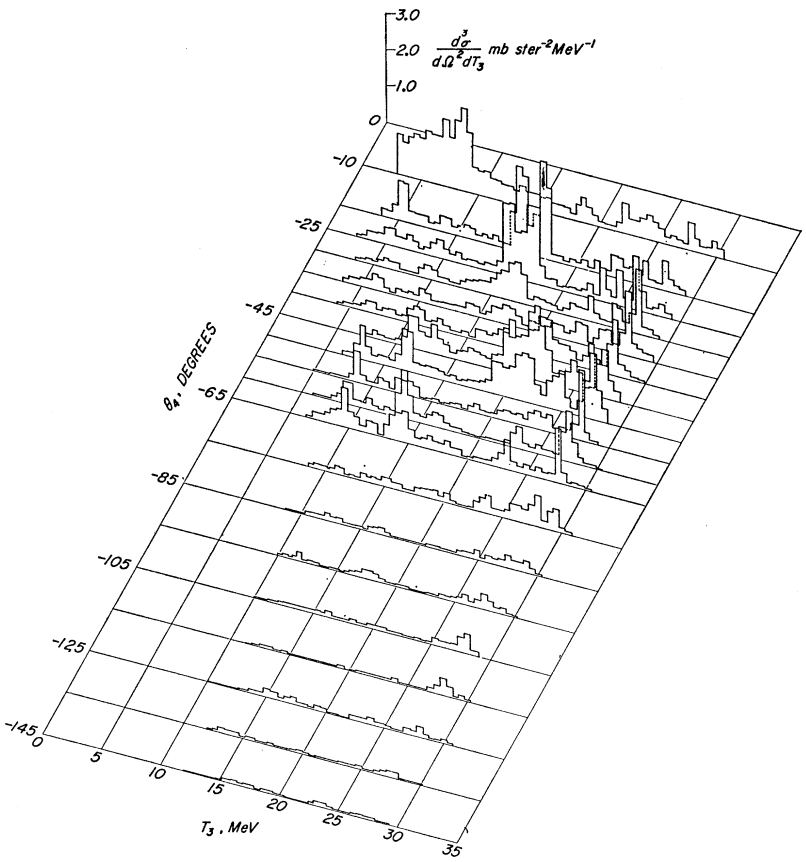

FIG. 11. A projection of T_3 spectra of the type of Fig. 10 taken at various angles θ_4. The energies T_3 have been corrected for target thickness.

band also is subtracted out. This, however, should affect only the absolute value of the measured cross-section and not its angular dependence.

After the contribution of the $O^{16}(\alpha,2\alpha)C^{12}{}_{g.s.}$ reaction had been isolated and the background subtracted, the numbers of events in the relevant T_4 channels for a given T_3 channel were added together. In each case a population histogram of the alpha-alpha band of the reaction $O^{16}(\alpha,2\alpha)C^{12}{}_{g.s.}$ was thus obtained as a function of T_3. It may be regarded as the projection of this band on the T_3 axis. Such an histogram is presented in Fig. 10 for the nominal detector angles $\theta_3=+25°$, $\theta_4=-25°$ and for $\theta_3=+25°$, $\theta_4=-23°$. As may be seen from Fig. 1, at these angles the allowed band on a T_3 versus T_4 diagram is well approximated at most energies by a straight line intercepting both T axes at an angle of 45°. In such a case, if θ_3 and θ_4 are symmetric, a projection of the type of Fig. 10 should clearly possess reflection symmetry about the point $T_3=T_4$, in this case for T_3 of about 16 MeV. The lack of this symmetry in Fig. 10 for the nominal angles $\theta_3=+25°$ and $\theta_4=-25°$, and the approximate symmetry seen at $\theta_3=+25°$, $\theta_4=-23°$ illustrates the error in the absolute angle reading. This error was reproducible during an entire angular correlation measurement and therefore was not too serious. Figure 10 also illustrates the great sensitivity of the cross sections to angle, which is all the more striking since the detectors had an angular width of about 4° each. Because of this angular sensitivity the uncertainties in angle are probably the largest single source of error in the experiment, in spite of all the precautions discussed above. Reproducibility checks indicated that the over-all absolute intensity accuracy of the experiment is about 30%, the gross features of the data being better reproducible than small details. The latter apparently depend on parameters such as the shape of the detectors which were not under sufficient control in the present experiment.

Histograms analogous to the ones presented in Fig. 10 were obtained for many angles θ_4, ranging from -10 to $-145°$, with θ_3 held constant at $+25°$. They were all corrected for target thickness and normalized to the differential cross section $d^3\sigma/dT_3 d\Omega_3 d\Omega_4$. They are presented in a projection in Fig. 11. The coordinates in this figure are T_3, θ_4, and the absolute differential cross section. The dependence of the energies of various peaks T_3 on the angle θ_4 should be compared to the kinematic diagrams of Fig. 3 and 4. The following features of these data may be noticed:

1. As evidenced by the prominent narrow peaks in Fig. 11, which often persist through a wide range of the angle θ_4, decaying states of O^{16} strongly influence the

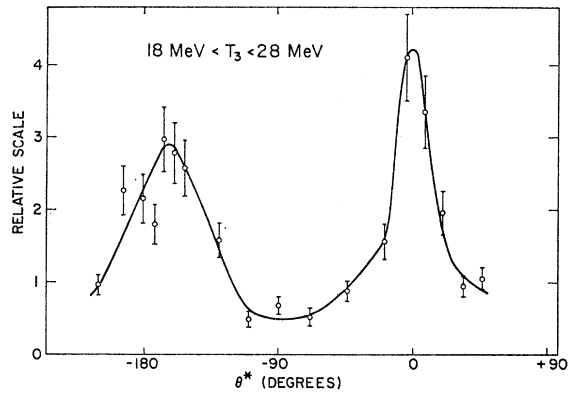

FIG. 12. The θ^* dependence of the intensity of that section of the ground-state alpha-alpha band which corresponds to the T_3 energy interval from 18 to 28 MeV.

reaction. Decaying states of Be^8 alone could never cause such violent modulations of the alpha-alpha bands for reasons discussed in Sec. III.[8] Some additional data were taken with smaller detector angular apertures, demonstrating that some peaks in the spectra are as narrow as 200 keV, equal to the experimental resolution.

2. From Fig. 11 it is apparent that the positions of peaks at high T_3 values tend to be independent of θ_4. On the other hand, at low T_3 values they vary in a systematic way, in agreement with the behavior of the family of curved bands in Fig. 3. This indicates that low-lying decaying states of O^{16} are preferentially excited. A detailed study of the spectrum taken at detector angles $+25°$, $-25°$ revealed that within the limited accuracy of energy and width determination of the present experiment, all the well-known low-lying natural-parity alpha-decaying states of O^{16} with spins 1 and 2 have their counterparts in this spectrum. The spin-zero state at 11.25 MeV is known to be too broad to be easily discernible. Conversely, the known 1^- and 2^+ states suffice to explain all definitely established peaks in the region of the $+25°$, $-25°$ spectrum corresponding to values Q_{int} up to about 16 MeV. Above that, the information on O^{16} states from other experiments is not sufficiently definite to make a comparison possible.

Insofar as the high T_3 part of Fig. 11 can be considered to be dominated by events in which the alpha particle from the decay of the intermediate O^{16} state is registered by detector 4, it represents an angular correlation between the alpha particle 3 involved in the first step, i.e., the excitation of O^{16}, and the alpha particle 4 emitted in the decay of the excited O^{16}. The lower T_3 part of Fig. 11 is dominated by events with the opposite time sequence and represents a complicated folding of the angular distribution of the first alpha particle (4) and its angular correlation with the subsequent alpha particle (3).

3. Even on the average, the population density of the T_3 versus θ_4 plane is far from uniform. The events tend rather to concentrate into "giant peaks": at T_3 of about 7 MeV around $\theta_4=-10°$, at T_3 of about 16 MeV around $\theta_4=-25°$, and at T_3 of about 24 MeV around $\theta_4=-50°$. Such giant peaks are not expected in the correlation pattern if the reaction mechanism is a pure two-step process. It can easily be seen from Fig. 4 that the giant peaks occur in the T_3 versus θ_4 graph in the region of small C^{12} recoil momentum. Additional measurements were performed in order to explore further this unexpected gross behavior of the angular correlation pattern. For this purpose a section of the ground-state alpha-alpha band corresponding to an energy interval in T_3 from 18 to 28 MeV was selected and the dependence on θ_4 of the differential cross section integrated over this energy interval was measured over a full circle of the angle θ_4. In the course of this measurement the distance of the moving detector 4 to the target was varied in such a way that the center-of-mass motion was compensated and the solid angle subtended by detector 4, as seen from the excited O^{16} nucleus, was always the same. It is possible to achieve this exactly only for a particular energy T_3, which was taken to be 23 MeV. The proper distance of detector 4 at each angle θ_4 can then be easily obtained from formulas given in Appendix II. This procedure yielded directly the relative differential cross section in the rest system of the moving intermediate O^{16} nucleus integrated over the chosen energy interval and the solid angles of the detectors. Because the angular correlation pattern is strongly intensity modulated, the yields are not directly proportional to the detector solid angles when these are as large as was the case in this series of measurements. Therefore, the procedure described above was found necessary in order to compare in a meaningful way the experimental results with the theoretical predictions mentioned in the Introduction.

Results obtained this way are presented in Fig. 12 as a function of the angle θ^* of the alpha particle emitted in the decay of the excited O^{16} nucleus. This angle is measured in the rest system of the excited O^{16} nucleus. $\theta^*=0$ has been chosen as the direction of the decay alpha particle when it coincides with the direction of the recoiling intermediate O^{16} nucleus in the laboratory system. If in the decay of the excited O^{16} nucleus the decay alpha particle is emitted in this direction, this alpha particle necessarily has the highest possible laboratory kinetic energy and therefore the laboratory kinetic energy of the associated recoiling C^{12} nucleus is the smallest. The error bars in Fig. 12 represent the estimated uncertainty at each point rather than statistical errors, which were in general smaller. The curve drawn through the experimental points is an estimate of the average behavior of the data.

There are several interesting features of this average

[8] In an experiment designed to detect coincidences between $C^{12}_{g.s.}$ recoil nuclei and both alpha particles from the decay of $Be^8_{g.s.}$, no such events were observed. The sensitivity of the measurement was sufficient to show that this reaction has a cross section very much smaller than that involving alpha-decaying states of O^{16}.

angular correlation. First, there is a strong and narrow peak in the laboratory direction of the excited O^{16} nucleus, i.e., the direction of highest laboratory momentum of the second alpha particle and smallest laboratory C^{12} recoil momentum. The symmetry prediction stated in the Introduction is nearly fulfilled in the sense that there is a peak in the back direction as well. However, the symmetry is clearly not perfect. The two peaks are not 180° apart and we believe that the deviation is outside experimental error. Also, the peak in the back direction is considerably broader than the peak in the forward direction. Another difference appears when one plots the energy spectra at the respective intensity maxima of the two peaks. These are shown in Fig. 13. Clearly the energy spectrum at the back maximum of the angular correlation pattern is better resolved into individual narrow levels than the energy spectrum at the forward maximum. All these features of the average correlation pattern are systematic in the sense that if one divides the energy interval in T_3 into two sections from 18–23 MeV and 23–28 MeV, these features persist in each half section.

One may also assume for the other two giant peaks noticed in Fig. 11 that the time sequence of the two alpha particles is such that the higher-energy alpha particle is emitted first. With this assumption one can calculate the approximate direction where a possible backward peak should appear. The respective backward peaks were indeed found but were not explored in any detail.

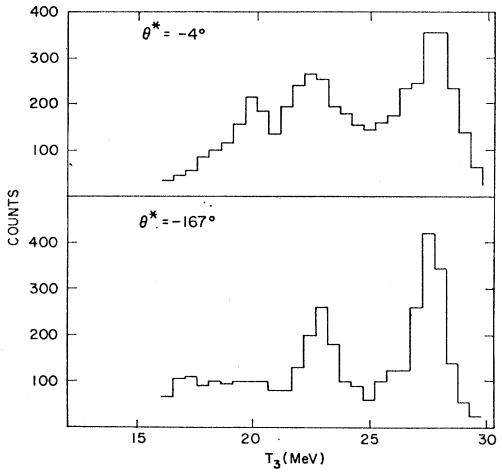

FIG. 13. T_3 spectra at the forward and backward intensity maxima of the angular-correlation pattern of Fig. 12.

V. DISCUSSION AND CONCLUSIONS

The salient characteristics of the experimental results just presented are the importance of the decaying states of O^{16}, and the dominant role of the laboratory momentum of the intermediate O^{16} system in determining the directions of gross maxima in angular correlation patterns. The latter phenomenon is theoretically most simply predicted if one describes the first step of the reaction, namely the inelastic scattering of the incident alpha particle as a direct process, treating it in plane-wave Born approximation. Assuming that the O^{16} nucleus consists of a $C^{12}{}_{g.s.}$ core and an alpha particle and that the interaction is a simple potential between the incident alpha particle and the alpha particle in the O^{16} nucleus, one can easily calculate the matrix elements for the process. Their angle-dependent parts are of the form:

$$\int e^{iA\cos\theta^*} Y_{lm}(\theta^*,\phi^*)\,\sin\theta^* d\theta^* d\phi^*.$$

Here A is a constant, θ^* and ϕ^* are polar angles of the vector connecting the alpha particle and the $C^{12}{}_{g.s.}$ core in the O^{16} nucleus, evaluated in a system with the z axis in the recoil direction. $Y_{lm}(\theta^*,\phi^*)$ is the angular part of the internal wave function of the excited O^{16} nucleus. Clearly only the matrix elements with $m=0$ are different from zero, i.e., only substates of O^{16} with $m=0$ are populated. The simplest assumption concerning the second step of the reaction would be that the states of O^{16} decay uninfluenced by the inelastically scattered alpha particle and without systematic phase correlations. Under these assumptions the average correlation between the inelastically scattered alpha particle and the alpha particle from the decay of the excited O^{16} nucleus should be of the form $\sum_l g_l P_l^2(\cos\theta^*)$ if the angle θ^* is measured in the rest system of the O^{16} excited nucleus with respect to the direction of the laboratory momentum of this nucleus. Here the P_l are Legendre polynomials, while the g_l are weighting factors for different angular momenta of the decaying O^{16} states, and are determined by the level distribution of O^{16} in the averaging interval. Assuming sufficiently large l values one could thus explain the narrow angular maximum in the direction of the laboratory momentum of the excited O^{16} nucleus. However, since low l values have been experimentally demonstrated to be of primary importance, one could not fit the large peak to valley ratio in the experimental angular correlation as shown in Fig. 12. Most important, no deviations from perfect symmetry could be expected.

One might try to save this simplest theoretical description by pointing out that the procedure used in this experiment for the separation of events with the correct time sequence of excitation and decay is not very precise. While this objection cannot be decidedly refuted on the basis of the present experiment alone, it is hardly probable that a cleaner separation procedure would restore complete symmetry. The known properties of the level structure of O^{16} in the energy region of interest and our general knowledge of the widths of alpha decaying states in light nuclei make a pure two-step description of the reaction $O^{16}(\alpha,2\alpha)C^{12}{}_{g.s.}$ at 40-MeV incident energy quite implausible. One should

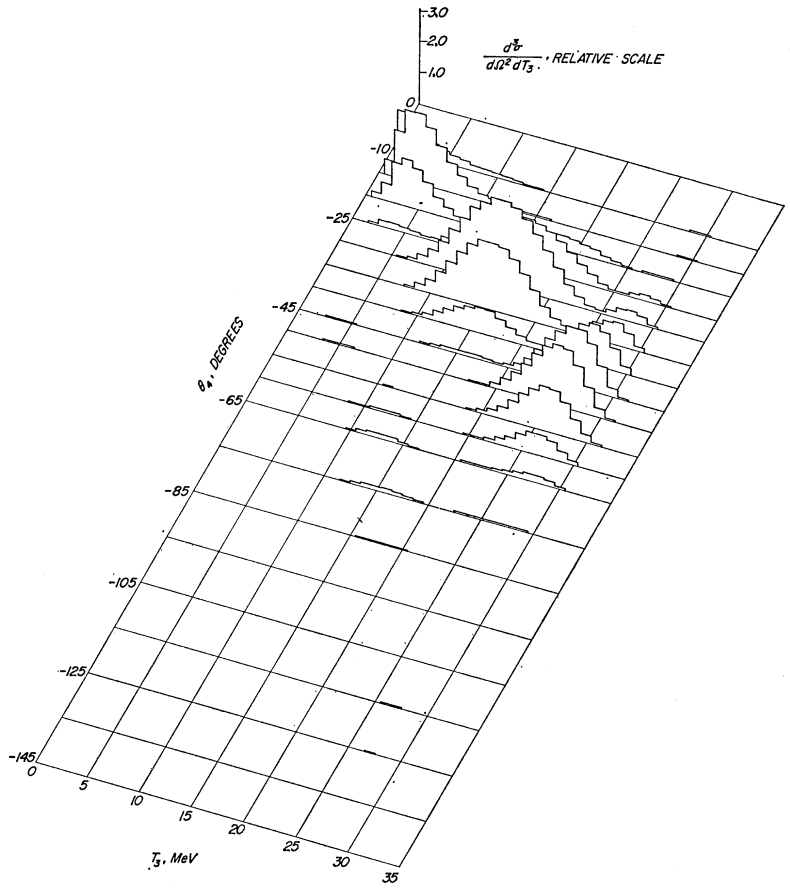

FIG. 14. A projection of the type of Fig. 11 of theoretical T_3 spectra at various angles θ_4.

rather expect the decay to follow the excitation in such short time intervals that final state interactions between any two of the outgoing particles should be important, and that the phases of intermediate states should be correlated. From this point of view it is actually surprising that the correlation pattern is as nearly symmetric as observed.

A detailed theory which would take all these three-body aspects of the reaction into account does not exist. If one wished to construct such a theory one would probably, as in many similar situations, try to start from solvable models and gradually introduce more complicated corrections. One possible starting point is the two-step model which was discussed above. The diametrically opposite simple picture is a knock-out process in the plane-wave Born approximation for both the incident particle and all outgoing particles. Here the incident and emitted alpha particles and the C^{12} nucleus are again considered to be elementary particles. All interactions between them are treated as first-order perturbations except the initial interaction in O^{16}, which is considered to be a bound system of one alpha particle and the $C^{12}{}_{g.s.}$ nucleus. In such a description obviously no intermediate systems or strong final state interactions are taken into account. On the other hand, since all three outgoing particles are treated on equal footing, such a treatment could provide a convenient starting point for a symmetric inclusion of final state interactions.

A calculation of this type for the reaction $O^{16}(\alpha,2\alpha)C^{12}{}_{g.s.}$ is outlined in Appendix III. For the perturbing potentials simple central two-body surface interactions between any pair of outgoing particles are introduced. The requirements of the indistinguishability principle with respect to the alpha particles outside the $C^{12}{}_{g.s.}$ nucleus are properly taken into account. The resulting expression for the differential cross section was evaluated on a computer using nuclear radii given by $r=r_0A^{1/3}$ and the simplest perturbing potential, namely a pure alpha-alpha interaction. The result, with $r_0=1.58$ fermis, is plotted in Fig. 14 in the same way as in Fig. 11 for direct comparison. While no fine structure can be expected in the computational result, one can, surprisingly enough, notice the appearance of the right number of "giant peaks" in approximately the right places. The sharp intensity modulation of the "giant peaks" in Fig. 11 illustrates in a striking fashion the importance of the interference between two-step and direct processes in the reaction. The resemblance between the gross features of the general intensity distribution of Fig. 11 and the prediction of the direct

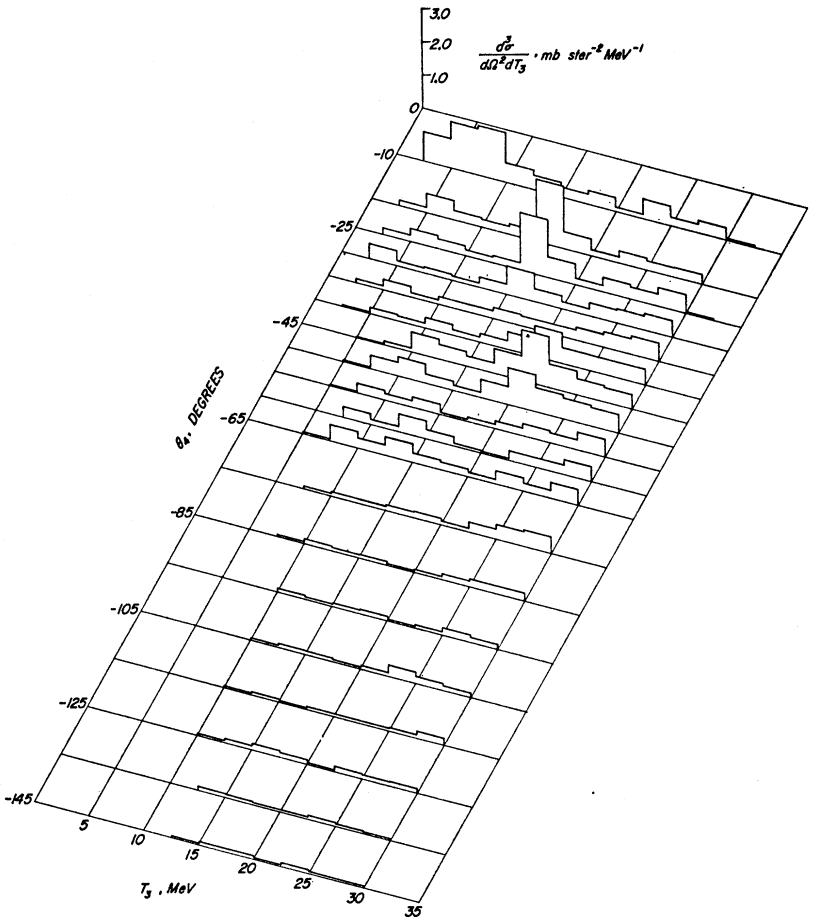

FIG. 15. A T_3 versus θ_4 plot showing the data of Fig. 11 with the T_3 coordinate summed over energy bins of 2.5 MeV.

knock-out theory as shown in Fig. 14 would be most clearly seen in an experiment done with poor energy resolution. Such an experiment has been simulated by summing the data of Fig. 11 in energy bins about 2.5 MeV wide. The result is shown in Fig. 15. The facts that only the simplest possible model has been evaluated and no parameters except r_0 have been adjusted make the resemblance of the theory to the experimental results quite remarkable.

Such a simple calculation cannot be expected to yield backward peaks. The situation is quite analogous to reactions with two outgoing particles, like stripping, where one is satisfied to fit the peak in the forward direction by a simple plane-wave theory, while any backward peaks are explained as distortion effects. Once distortion effects were introduced in the present context one would be well under way toward a more realistic three-body treatment of the reaction. At present there seems to be no simple criterion for deciding which simplifications should be introduced into such a treatment, apart from the completely arbitrary criterion of mathematical feasibility. More experience gained with reactions similar to $O^{16}(\alpha,2\alpha)C^{12}_{g.s.}$ may bestow upon us sufficient physical intuition to point a way through the forest of mathematical difficulties.

Even the present scanty results indicate that studies of reactions with three outgoing particles might be used for the accumulation of spectroscopic data on two-body intermediate systems in spite of the inextricable knock-out features of such reactions. There should exist regions of energy and angle where the knock-out aspects are of little importance. For instance, one might expect that the knock-out mechanism should favor coplanar events. Experimental configurations with the two detectors not coplanar with the beam might thus be better analyzable in terms of pure two-step mechanisms than the results presented in this paper. Some confirmation of this expectation has been obtained recently.[9] A kinematically more complete investigation of a reaction with three outgoing particles is needed to determine the general correctness of this conjecture. Recent progress in experimental technique, especially in data-handling procedures, may now have made such investigations feasible.

ACKNOWLEDGMENTS

The cooperation of the members of the Cyclotron crew, C. Glover, J. Hessinger, H. Maloney, and M.

[9] R. A. Lasalle, J. G. Cramer, Jr., and W. W. Eidson, Phys. Letters **5**, 170 (1963).

Petruk is gratefully acknowledged. Special thanks are due Dr. Maurice Goldhaber and Dr. Walter Brown for their continued interest in the present work and many discussions, and to Mrs. Betty Phillips for her energy and forbearance in the assembling and typing of this paper.

APPENDIX I

In the following, the derivation of the selection rule of A. Bohr[3] is recapitulated and applied in the present context. The argument is simplified by the fact that all ingoing and outgoing particles in the reaction $O^{16}(\alpha,2\alpha)C^{12}{}_{g.s.}$ have zero spin. The first step of the reaction, i.e., the incidence of an alpha particle onto a target consisting of O^{16} nuclei in their ground states and the subsequent observation of an inelastically scattered alpha particle with a definite momentum, can be considered as the preparation of a certain excited state of O^{16}. Only the natural parity states of O^{16} are of interest, since only these can decay into an alpha particle and $C^{12}{}_{g.s.}$. The preparation process obviously possesses a plane of reflection symmetry, namely, the scattering plane defined by the incident beam and the direction of the inelastically scattered alpha particle. The state of O^{16} prepared in this way cannot thus be affected by such a reflection, i.e., it must be an eigenstate of the operator R which effects the reflection. This operator is the product of the usual parity operator Π and the operator for rotation by 180° around the normal to the scattering plane $e^{i\pi J_z}$, J_z being the component of the total angular momentum along the normal: $R=\Pi e^{i\pi J_z}$. Since $R^2=1$, the only possible eigenvalues of the operator R are $+1$ and -1.

In the rest system of the excited O^{16} nucleus the relevant wave function is the internal wave function of this nucleus. Quantizing in this system the excited state of O^{16} along the normal to the scattering plane, the angular part of its internal wave function is of the form $\sum_M a_M Y_{LM}(\vartheta,\varphi)$. The $Y_{LM}(\vartheta,\varphi)$ are spherical harmonics of the polar angles ϑ and φ, while the a_M are constant coefficients determined by the details of the excitation process with the following restriction: Since the parity and angular momentum are conserved in a nuclear reaction, and $R=\Pi e^{i\pi J_z}$, the R eigenvalue of the excited state of O^{16} must be the same as that of the initial ground state of O^{16}, $+1$. We have $RY_{LM}=(-1)^{L+M}Y_{LM}$. Thus, only even terms enter into the wave function $\sum_M a_M Y_{LM}(\vartheta,\varphi)$ if the parity of the excited state is even, and only odd terms if the parity is odd. The angular pattern of the decay products of the excited O^{16} nucleus in its rest system is entirely determined by the square of the absolute value of the angular wave function, and is therefore of the form $|\sum_M a_M Y_{LM}(\vartheta,\varphi)|^2$. Writing $Y_{LM}(\vartheta,\varphi)=\Theta_{LM}(\varphi)e^{iM\varphi}$ where $\Theta_{LM}(\vartheta)$ is a function of the angle ϑ only, one sees that the angular pattern is in any case a function of the parameters ϑ and 2φ. Thus, it is periodic in φ with a period of 180° and the normal to the scattering plane is an axis of twofold rotational symmetry for the decay products. (The angle φ is the angle referred to as θ^* in the main body of the text.) This symmetry is not affected if several states of the same parity overlap. In general the symmetry disappears, however, if states of opposite parity overlap at the energy of interest.

APPENDIX II

In the transition from an inertial system S to an inertial system S', which moves with respect to S with a velocity $\mathbf{v}$, the velocity $\mathbf{v}_i$ of particle i transforms into the velocity $\mathbf{v}_i'$ given by

$$\mathbf{v}_i'=\mathbf{v}_i-\mathbf{v}. \tag{1}$$

The transformation of kinetic energies is obtained by observing that in any inertial system the kinetic energy is given by $T_i=m_i v_i^2/2$, m_i being the invariant mass of particle i. The angle θ_i between the direction of particle i and the direction of the system velocity $\mathbf{v}$ is transformed in such a way that

$$\cot\theta_i'=\cot\theta_i-\frac{|\mathbf{v}|}{|\mathbf{v}_i|}\frac{1}{\sin\theta_i}. \tag{2}$$

This equation follows in a straightforward way from Eq. (1). In our case, all velocity vectors of interest lie in a plane. The angles θ_i and θ_i' may be considered to be defined by their magnitudes and signs, the magnitudes being restricted to the interval from 0 to 180°. The signs are obviously invariant under the transition to the system S'. Thus, Eq. (2) completely defines the transformation properties of θ_i.

The transformation properties of the product of solid angle and energy differentials $d\Omega_3 d\Omega_4 dT_3$ are obtained by observing that the quantity

$$\frac{p_3 p_4 d\Omega_3 d\Omega_4 dT_3}{1-(\mathbf{v}_4\cdot\mathbf{v}_5/v_4^2)}$$

is the result of the integration of the manifestly Galilean invariant quantity

$$\delta^3(\mathbf{p}_1+\mathbf{p}_2-\mathbf{p}_3-\mathbf{p}_4-\mathbf{p}_5)\times\delta(T_1+T_2+Q-T_3-T_4-T_5)d\mathbf{p}_3 d\mathbf{p}_4 d\mathbf{p}_5$$

with respect to $\mathbf{p}_5$ and T_4, and is therefore itself a Galilean invariant. The only precaution to be taken is to avoid those combinations of variables for which the expression in the denominator is zero. This never occurs in the region of interest for the present experiment.

The inertial system S' in which the intermediate nucleus formed by particles 4 and 5 is at rest is defined by $p_{45}'=0$. Its velocity $\mathbf{v}$ with respect to the laboratory system S is given by $\mathbf{v}=\mathbf{p}_{45}/m_{45}$.

Thus the product of solid angle and energy differentials in the moving (primed) frame is given by

$$d\Omega_3' d\Omega_4' dT_3'=\left[\frac{1-(\mathbf{v}_4'\cdot\mathbf{v}_5'/v_4'^2)}{1-(\mathbf{v}_4\cdot\mathbf{v}_5/v_4^2)}\right]\frac{p_3 p_4}{p_3' p_4'}d\Omega_3 d\Omega_4 dT_3.$$

APPENDIX III

In a simple plane-wave-Born-approximation treatment of the knock-out process with spinless incoming and outgoing particles, the initial and final states are described by wave functions

$$\psi_i=\exp(i\mathbf{p}_1\cdot\mathbf{r}_a)\exp(i\mathbf{p}_2\cdot\mathbf{R})\Phi(\boldsymbol{\varrho}),$$
$$\psi_f=\exp(i\mathbf{p}_3\cdot\mathbf{r}_a)\exp(i\mathbf{p}_4\cdot\mathbf{r}_b)\exp(i\mathbf{p}_5\cdot\mathbf{r}_c),$$

with $\mathbf{R}=(m_b\mathbf{r}_b+m_c\mathbf{r}_c)/(m_b+m_c)$ and $\boldsymbol{\varrho}=\mathbf{r}_b-\mathbf{r}_c$. We put $\hbar=1$. For the moment all three particles involved, labeled a, b, c, are considered different. One has $\mathbf{p}_1+\mathbf{p}_2=\mathbf{p}_3+\mathbf{p}_4+\mathbf{p}_5$ and the kinematics is as described elsewhere in this paper. In the initial state the particles b and c are considered bound in a relative s state. Their state of internal motion is described by the wave function $\Phi(\boldsymbol{\varrho})$, normalized so that $\int\Phi\Phi^*d\boldsymbol{\varrho}=1$. The perturbing potential is assumed to be a sum of central two-body potentials

$$V=V_{ab}(|\mathbf{r}_a-\mathbf{r}_b|)+V_{ac}(|\mathbf{r}_a-\mathbf{r}_c|).$$

The evaluation of matrix element $\langle\psi_f|V|\psi_i\rangle$ yields

$$\langle\psi_f|V|\psi_i\rangle=(2\pi)^3\delta^3(\mathbf{p}_1+\mathbf{p}_2-\mathbf{p}_3-\mathbf{p}_4-\mathbf{p}_5)$$
$$\times\Big\{\int\exp[i(\mathbf{p}_1-\mathbf{p}_3)\cdot\mathbf{r}]V_{ab}(\mathbf{r})d\mathbf{r}$$
$$+\int\exp(i\mathbf{q}\cdot\boldsymbol{\varrho})\Phi(\boldsymbol{\varrho})d\boldsymbol{\varrho}$$
$$+\int\exp[i(\mathbf{p}_1-\mathbf{p}_3)\cdot\mathbf{r}]V_{ac}(\mathbf{r})d\mathbf{r}$$
$$\times\int\exp(i\mathbf{Q}\cdot\boldsymbol{\varrho})\Phi(\boldsymbol{\varrho})d\boldsymbol{\varrho}\Big\}$$

with $\mathbf{q}=\mathbf{p}_1+[m_b/(m_b+m_c)]\mathbf{p}_2-\mathbf{p}_3-\mathbf{p}_4$ being the momentum transferred in the reaction to particle c, and $\mathbf{Q}=\mathbf{p}_1+[m_c/(m_b+m_c)]\mathbf{p}_2-\mathbf{p}_3-\mathbf{p}_5$ being the momentum transferred to particle b. If the particles a and b are identical bosons, the initial and final wave functions must be symmetrized with respect to them. As far as the matrix element is concerned this is equivalent to a symmetrization of the potentials and the symmetrization of the matrix element with respect to the momenta $\mathbf{p}_3$ and $\mathbf{p}_4$. One gets thus

$$\langle\psi_b|V|\psi_i\rangle=(2\pi)^3\delta^3(\mathbf{p}_1+\mathbf{p}_2-\mathbf{p}_3-\mathbf{p}_4-\mathbf{p}_5)M,$$

with

$$M=\int\{\exp[i(\mathbf{p}_1-\mathbf{p}_3)\cdot\mathbf{r}]+\exp[i(\mathbf{p}_1-\mathbf{p}_4)\cdot\mathbf{r}]\}V_{aa}(\mathbf{r})d\mathbf{r}$$
$$\times\int\exp(i\mathbf{q}\cdot\boldsymbol{\varrho})\Phi(\boldsymbol{\varrho})d\boldsymbol{\varrho}$$
$$+\int\exp[i(\mathbf{p}_1-\mathbf{p}_3)\cdot\mathbf{r}]V_{ac}(\mathbf{r})d\mathbf{r}$$
$$\times\int\exp(i\mathbf{Q}_4\cdot\boldsymbol{\varrho})\Phi(\boldsymbol{\varrho})d\boldsymbol{\varrho}$$
$$+\int\exp[i(\mathbf{p}_1-\mathbf{p}_4)\cdot\mathbf{r}]V_{ac}(\mathbf{r})d\mathbf{r}$$
$$\times\int\exp(i\mathbf{Q}_3\cdot\boldsymbol{\varrho})\Phi(\boldsymbol{\varrho})d\boldsymbol{\varrho}.$$

Here V_{aa} is the perturbing interaction between the two identical bosons and V_{ac} the perturbing interaction between either of them and particle c. $\mathbf{Q}_4$ and $\mathbf{Q}_3$ are defined by $\mathbf{Q}_4=\mathbf{p}_1+[m_c/(m_a+m_c)]\mathbf{p}_2-\mathbf{p}_3-\mathbf{p}_5$ and $\mathbf{Q}_3=\mathbf{p}_1+[m_c/(m_a+m_c)]\mathbf{p}_2-\mathbf{p}_4-\mathbf{p}_5$. The cross section may be expressed in terms of this matrix element by

$$d\sigma=\frac{m_a}{(2\pi)^5\mu}\int|M|^2\delta^3(\mathbf{p}_1+\mathbf{p}_2-\mathbf{p}_3-\mathbf{p}_4-\mathbf{p}_5)$$
$$\times\delta(T_1+T_2+Q-T_3-T_4-T_5)d\mathbf{p}_3d\mathbf{p}_4d\mathbf{p}_5$$
$$=\frac{m_a^2}{(2\pi)^5\mu}|M|^2\frac{p_3p_4d\Omega_3d\Omega_4dT_3}{1-(\mathbf{v}_4\cdot\mathbf{v}_5/v_4^2)};$$

here $\mu=\{(\mathbf{v}_1-\mathbf{v}_2)^2-(\mathbf{v}_1\times\mathbf{v}_2)^2\}^{1/2}$. If the denominator happens to be zero, it is simplest to integrate the theoretical cross section with respect to T_3 instead of T_4. It is easily seen that both procedures cannot yield a zero denominator simultaneously.

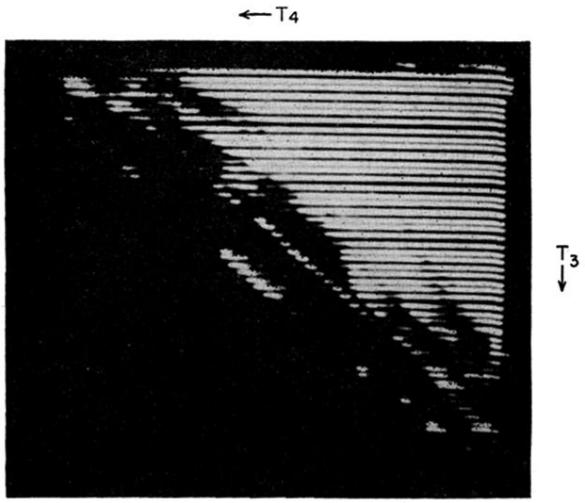

FIG. 6. A cathode-ray-tube display of raw data stored in the two-dimensional analyzer from the reaction $O^{16}(\alpha,2\alpha)C^{12}$ at detector angles $\theta_3=+25°$, $\theta_4=-25°$. See text for complete explanation of figure.

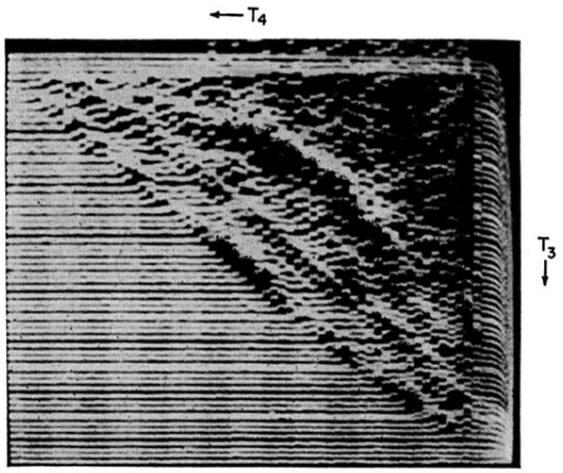

FIG. 7. A cathode-ray-tube display of raw data stored in the two-dimensional analyzer from the reaction $O^{16}(\alpha,2\alpha)C^{12}$ at detector angles $\theta_3=+25°$, $\theta_4=-25°$. See text for complete explanation of figure.

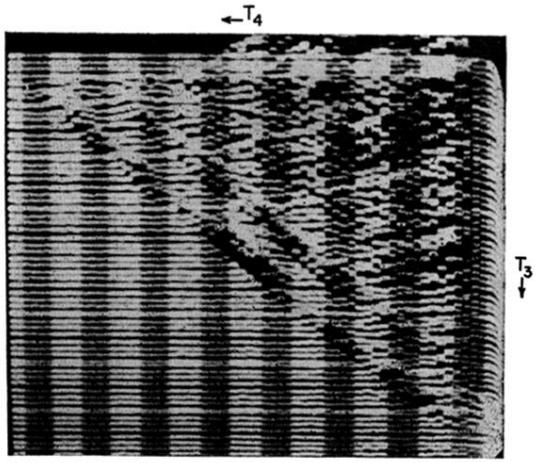

FIG. 8. A cathode-ray-tube display of raw data stored in the two-dimensional analyzer from the reaction $O^{16}(\alpha,2\alpha)C^{12}$ at detector angles $\theta_3=+25°$, $\theta_4=-25°$. See text for complete explanation of figure.